ISSN: 2230-9926

Available online at http://www.journalijdr.com

IJDR

International Journal of Development Research
Vol. 12, Issue, 11, pp. 60041-60050, November, 2022
https://doi.org/10.37118/ijdr.25653.11.2022

CASE REPORT OPEN ACCESS

USE OF ARTIFICIAL INTELLIGENCE IN NEURO-OPHTHALMOLOGICAL DIAGNOSIS: LEARNING FROM REAL DATA AND DEVELOPMENT OF METHODS TO ADDRESS CURRENT AND FUTURE CHALLENGES

***[1]João Gabriel Mendes de Oliveira da Rocha, [1]Gabriel Chaves Chaves, [1]Gabriela Medeiros de Mendonça, [2]Wilson Dahas Jorge Neto, [1]Luis Fernando Praia Rodrigues, [1]Vinícius de Almeida Rodrigues da Silva e Souza, [1]Sandro Cavalcante Raiol, [2]Lucas Coutinho Tuma da Ponte, [1]Leonardo Quirino Da Silva Reis and [1]Maria Luiza Del Tetto Zaccardi**

[1]Centro Universitário do Pará (CESUPA), Pará, Brazil; [2]Universidade Estadual do Pará (UEPA), Pará, Brazil

ARTICLE INFO

Article History:
Received 20th August, 2022
Received in revised form
24th September, 2022
Accepted 27th October, 2022
Published online 30th November, 2022

Key Words:
Computer vision system, Ophthalmoscopies, Pattern recognition, Ophthalmology.

****Corresponding author:***
João Gabriel Mendes de Oliveira da Rocha

ABSTRACT

It is important to have a critical view of the support provided by Artificial Intelligence (AI) in medical context, in order to trust this support. The objective was to measure/compare unidimensional uncertainty of an AI and a human performing the same task by a cross-sectional study. It was given to a simple algorithm written in Python (blob detection, OpenCV) and to an ophthalmologist the task of detecting a two-dimensional pattern (center of the optical disc) in 1,000 digital images of normal/abnormal fundoscopies. Algorithm performed the task 1x, human performed the task 2x, both using digital register of spatial coordinates. Machine's unidimensional level of uncertainty was measured by the respective comparison of the x and y coordinates recorded by machine and human. Human's unidimensional level of uncertainty was measured by comparing the coordinates recorded by human itself. Data analysis was performed using R AI failed to detect the target pattern onlyin two images. On average, man and machine showed a higher level of uncertainty in the ycoordinates, which was greater (~100 units) in machine's performance. The measure of uncertainty of AI and humans in the same task can help understand AI limitations and define its usefulness as a medical support tool.

Citation: João Gabriel Mendes de Oliveira da Rocha, Gabriel Chaves Chaves, Gabriela Medeiros de Mendonça, Wilson Dahas Jorge Neto, Luis Fernando Praia Rodrigues, Vinícius de Almeida Rodrigues da Silva e Souza, Sandro Cavalcante Raiol, Lucas Coutinho Tuma da Ponte, Leonardo Quirino Da Silva Reis and Maria Luiza Del Tetto Zaccardi, 2022. *"*Use of artificial intelligence in neuro-ophthalmological diagnosis: learning from real data and development of methods to address current and future challenges*", International Journal of Development Research, 12, (11), 60041-60050.*

INTRODUCTION

In the 1990s, a major paradigm shift emerged in medical diagnosis, entitled Evidence-Based Medicine, in which there was a proposal to include Clinical Epidemiology data in the professional decision-making process, previously dominated by semiology and propaedeutics isolated from the organization of the science by Hippocrates. From this period onwards, scientific journals, books and medical conferences disseminated statistical terms such as Accuracy, Sensitivity, Specificity, Positive Predictive Value, Likelihood Ratio, Odds Ratio, Relative Risk, Number Needed to Treat and many others. We all had to adapt to this more precise medicine, both within the scope of research and in our daily work with the patient[1]. In recent years, a new revolution is taking place, the inclusion of the so-called Artificial Intelligences (AI) in the Health area.

The need to learn to deal with these new tools, understand their concepts, metrics, applications and limitations already exist today. In several daily activities, from the use of a GPS application, text translation, or a simple search for terms in a browser, AI is already inserted, now, new applications have emerged in the field of Ophthalmology, such as IDx-DR, first automated diagnostic tool authorized by the Food and Drugs Administration (FDA) to perform the prediction of Diabetic Retinopathy through Retinography[2]. AI was conceptualized in 1956 after a workshop at Dartmouth College. The term Machine Learning (ML) was later used by Arthur Samuel in 1959 who stated "The computer must have the ability to learn using various statistical techniques, without being explicitly programmed". Using ML, the algorithm can learn and make predictions based on the data that was fed into the training phase, using either a supervised or unsupervised approach method. ML has been widely adopted in applications such as computer vision and predictive analytics using complex mathematical models. With the advent of graphics

processing units (GPUs), advances in mathematical models, the availability of large data sets and low-cost sensors, deep learning techniques - Deep learning (DL) - subsequently aroused fierce interest and were applied in many sectors. Thus, with the help of AI, professionals can reduce the costs of specialized care, in addition to the benefit of sharing the use of information systems, since the data generated by patient care can be aggregated and organized, producing a context that will also support the decision-making process. automated image recognition[4]. Decisions regarding patient treatment generating a direct impact on cost reduction in the health area[3,4]. AI offers a beacon of hope to improve some of the gaps inherent in human-operated healthcare including misdiagnosis, wasted resources and insufficient doctor-patient time resulting from the imbalance between demand and supply. Advances in AI have the potential to create wavefronts through teleophthalmology pathways in national health services. Automated image recognition allows computers to analyze and process retinal images and subsequently distinguish lesions through guideline scales previously learned by the AI algorithm. There is promise that the connection between AI and teleophthalmology will strengthen benchmarks and improve patient care[4]. AI involves DL through datasets without explicit programming, and DL involves additional self-training using "artificial neural networks". DL involves identifying a correlation between data in large neural networks in the data sets. Within image-based specialties such as ophthalmology, convolutional neural networks use labeled data to recognize patterns, with published evidence of their capabilities for diabetic retinopathy, glaucoma and retinopathy of prematurity and age-related macular degeneration, and even analyzing their clinical application. in cataract screening[5].

MATERIALS AND METHODS

This project was approved by the Ethics Committee for Research with Human Beings (CAAE: 39292420.2.0000.5169). It is configured as a descriptive, analytical, observational and cross-sectional study, and is part of a line of research, which in addition to statistically comparing the performance of the AI tool with the ophthalmologist, aims to identify, propose corrections to the limitations of AI and develop new ones. proposed a tool in the evaluation of neuro-ophthalmological data. All data that were used in this project are contained in the files of RedCheck (Annex 1), a collaborating institution in this Project. The nature of the data is numerical and/or categorical, being relative to the results of normal fundus examinations (n = 500) and altered by different neuro-ophthalmological diseases (n = 500). The machine was fed with 1000 funduscopies to detect the center of the optic disc. Initially the image in JPEG format is converted from the BGR format to RGB, where the primary colors that make up each pixel (Red, Green and Blue) are reordered in their annotation. Then the image is converted to grayscale. Next, a dynamic threshold is applied to the grayscale image, basically, the value of each pixel is checked and in case it is above a threshold, it is increased to the maximum value (becoming completely white), and if is lower, it is reduced in value to the minimum (becoming completely black).

In this way, on the image with applied threshold, the search of the optical disc region is performed through a Computer Vision method called SimpleBlobDetector, present in a free access library called OpenCV created by Intel®. If not found, the threshold cut-off values are adjusted again until the region is found or not. This method above finds regions (Contours) of pixels that maintain some relationship with each other due to their color characteristics, segmenting the image into its components. The Center for these components is found and registered. In order to be characterized as an Optical Disk, the contour in question must comply with some arbitrarily defined characteristics: 1 – A minimum area of 1 thousand pixels and a maximum of 10 thousand pixels; 2 – A minimum circularity of 0.1; 3 – A minimum convexity of 0.1. The detection of the optic disc center was represented with the generation of 'X' coordinates and 'Y' coordinates from a Cartesian plane. There is no need for training, and the computational cost is low because it does not use artificial neural networks. Thus, considering the proposal to use a technique for preliminary screening of the Optical Disc region, it appears as a possible methodological option, in addition the technique can be applied in series or parallel with other methods to refine the accuracy. An experienced ophthalmologist volunteered in the same task, ie, to detect and digitally mark with a cursor the center of the optic disc in the same funduscopy images. Using the 1000 funduscopies, 500 normal and 500 with various ophthalmological alterations, from the Red Check database, the ophthalmologist marked all the retinographies at first, and later marked them again, recording other data for comparative analysis with the first ones.

When it is intended to evaluate the agreement between two methods that should measure the same amount, analyzes are used that are not always correct. It is important that the use of correlation is avoided in these situations and that the methodology is used properly, including the limits of agreement and their confidence intervals, in addition to commenting on whether the limits found are acceptable differences from a clinical point of view. The analysis of agreement between Bland-Altman methods is suitable for this comparison, precisely because it allows the comparison between means of results obtained with different measurement methods and the difference of results obtained by different methods (Bland-Altman, 1983). Data analysis was performed using the R statistical computing program (www.r-project.org). from these coordinates, concordance analyzes were performed using the Bland-Altman and correlation calculations, generating comparative graphs in: 1st ophthalmologist observation versus 2nd ophthalmologist observation 'X' coordinate of normal funduscopy, 1st ophthalmologist observation versus 2nd observation ophthalmologist's 'Y' coordinate of normal funduscopies, 1st ophthalmologist observation versus 2nd ophthalmologist's observation 'X' coordinate of altered funduscopies, 1st ophthalmologist's observation versus 2nd ophthalmologist's observation 'Y' coordinated of altered funduscopies, 1st ophthalmologist's observation versus 2nd ophthalmologist's observation 'X' coordinated of normal together with altered funduscopy, 1st ophthalmologist's observation versus 'Y'-coordinated ophthalmologist's observation of normal together with altered funduscopies, 1st ophthalmologist observation versus 'X' coordinate machine in normal funduscopies, 1st ophthalmologist observation versus 'Y' coordinate machine in normal funduscopies, 1st ophthalmologist observation versus 'X' coordinate machine in funduscopies altered, 1st ophthalmologist observation versus 'Y' coordinate machine in altered funduscopies, 1st ophthalmologist observation versus 'X' coordinate machine in normal and altered funduscopies, Ophthalmologist's 1st observation versus 'Y' coordinate machine on normal and altered funduscopies, ophthalmologist's 2nd observation versus 'X' coordinate machine on normal funduscopies, ophthalmologist's 2nd observation versus 'Y' coordinate machine on normal funduscopies, 2nd observation of the ophthalmologist versus the 'X' coordinate machine in altered funduscopies, 2nd observation by the ophthalmologist versus the 'Y' coordinated machine in altered funduscopies, 2nd observation by the ophthalmologist versus the 'X' coordinated machine in normal together with altered funduscopies, 2nd observation by the ophthalmologist versus the 'Y' coordinate machine in normal and altered funduscopies.

RESULTS

In all graphs, the correlation analysis was strong, whereas the degree of agreement test had variations in the average differences of up to approximately 100 units. In the graphs of the ophthalmologist's 1st observation versus the ophthalmologist's 2nd observation 'X' coordinate with normal funduscopy, the correlation between the observations was strong (Figure 1) and the mean difference in the Bland-Altman analysis (Figure 2) was close to 0, showing good agreement. In the graphs of the 1st ophthalmologist's observation versus the 2nd ophthalmologist's observation 'Y' coordinate with normal funduscopies, the correlation was strong (Figure 3) and the mean difference was close to 0 in the concordance analysis (Figure 4). In the graphs of the 1st ophthalmologist's observation versus the 2nd ophthalmologist's observation 'X' coordinate with altered funduscopies, the correlation was strong (Figure 5) and the mean difference was close to 0 (Figure 6).

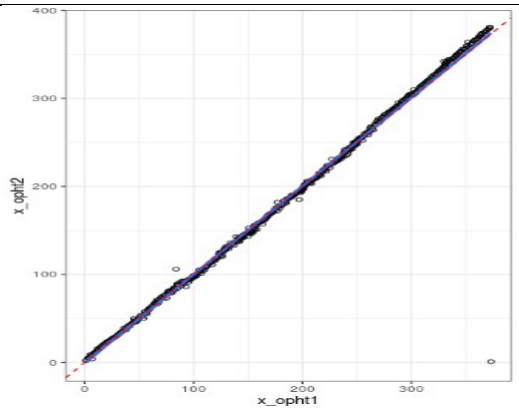

Figure 1. Correlation between the 1st and 2nd observation by the ophthalmologist X coordinate in normal funduscopies. R=0.96

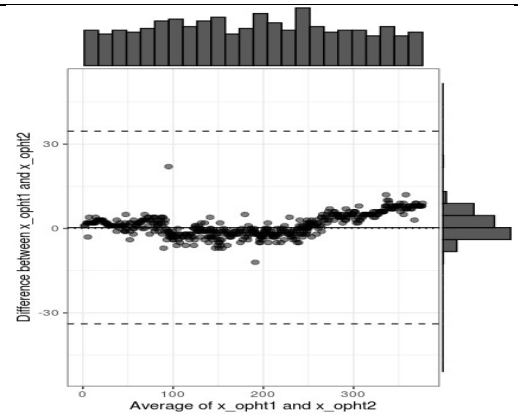

Figure 2. Degree of agreement between the 1st and 2nd observation by the ophthalmologist X coordinate in normal funduscopies

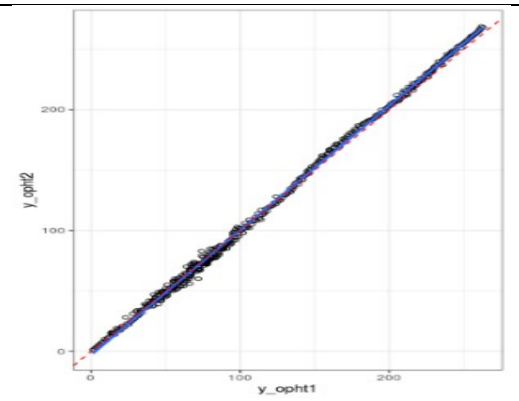

Figure 3. Correlation between the 1st and 2nd observation by the ophthalmologist Y coordinate in normal funduscopy. R=0.96

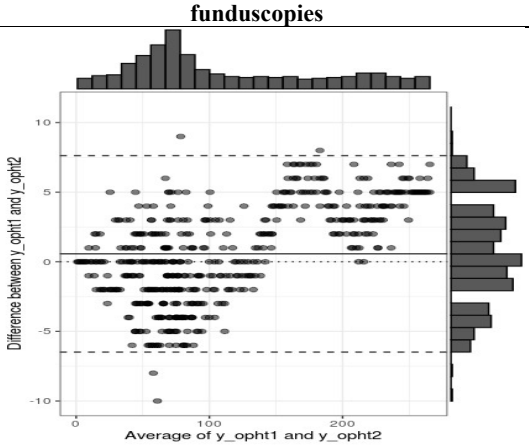

Figure 4. Degree of agreement between the 1st and 2nd observation by the ophthalmologist Y coordinate in normal funduscopies

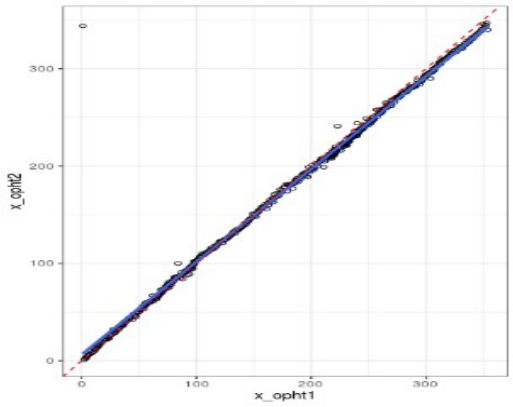

Figure 5. Correlation between the 1st and 2nd observation by the ophthalmologist X coordinate in altered funduscopies. R=0.96

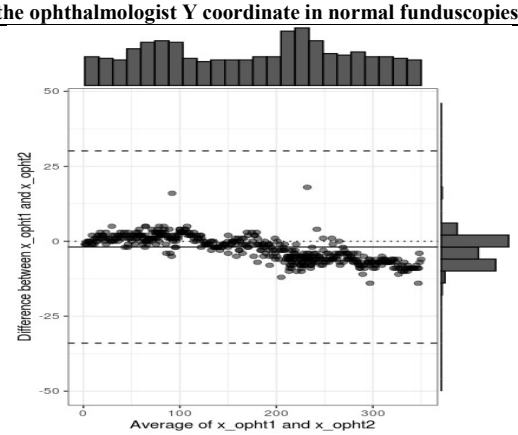

Figure 6. Degree of agreement between the 1st and 2nd observation of the ophthalmologist coordinate X in altered funduscopies

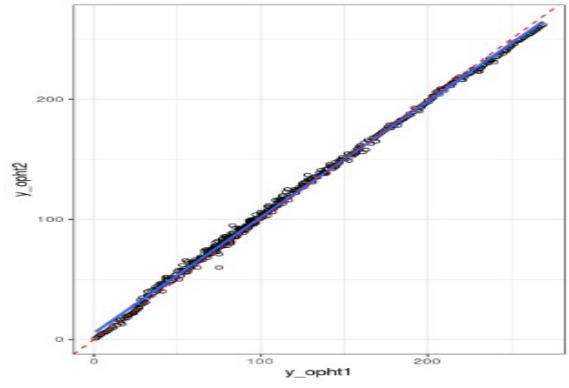

Figure 7. Correlation between the 1st and 2nd observation of the ophthalmologist coordinate Y on altered funduscopies. R=0.96

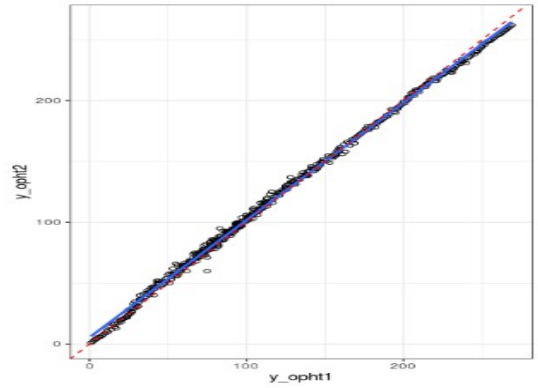

Figure 8. Degree of agreement between the 1st and 2nd observation by the ophthalmologist Y coordinate in altered funduscopies

In the graphs of the 1st ophthalmologist's observation versus the 2nd ophthalmologist's observation 'Y' coordinate with altered funduscopies, the correlation was strong (Figure 7) and the mean difference in the concordance analysis was approximately 1.25 (Figure 8). In the graphs of the 1st ophthalmologist's observation versus the 2nd ophthalmologist's observation 'X' coordinate with normal funduscopies together with altered funduscopy, the correlation was strong (Figure 9) and the mean difference approached 0 (Figure 10). In the graphs of the 1st ophthalmologist's observation versus the 2nd ophthalmologist's observation 'Y' coordinate with normal and abnormal funduscopies, the correlation was strong (Figure 11) and the mean difference was around 8 units above 0 (Figure 12).

In the graphs of the ophthalmologist's 1st observation versus the 'X' coordinate machine in normal funduscopy, the correlation was strong (Figure 13), whereas the mean difference was about 35 units above 0 in the agreement analysis (Figure 14). In the graphs of the ophthalmologist's 1st observation versus the 'Y' coordinate machine in normal funduscopy the correlation was strong (Figure 15) and the mean difference was about 50 units above 0 (Figure 16). In the graphs of the ophthalmologist's 1st observation versus the 'Y' coordinate machine in normal funduscopy the correlation was strong (Figure 15) and the mean difference was about 50 units above 0 (Figure 16). In the graphs of the 1st observation of the ophthalmologist versus the 'Y' coordinate machine in altered funduscopies, the correlation was

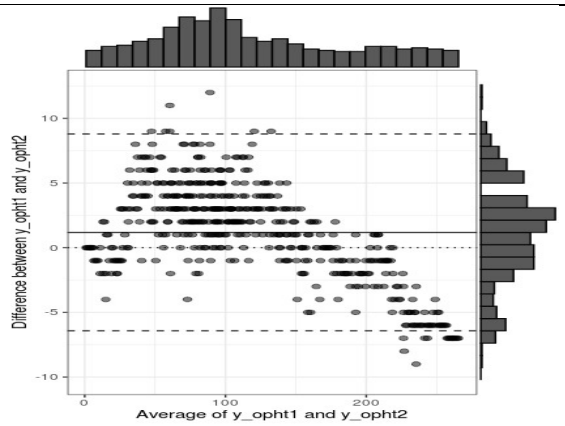

Figure 9. Correlation between the 1st and 2nd observation by the ophthalmologist X-coordinated in normal and abnormal funduscopies. R=0.96

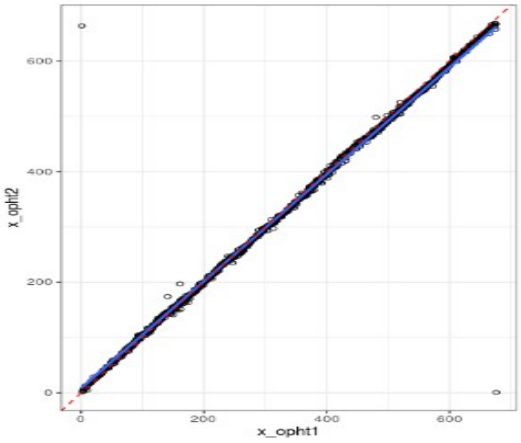

Figure 10. Degree of agreement between the 1st and 2nd observation by the ophthalmologist coordinate X in normal funduscopies together with altered ones

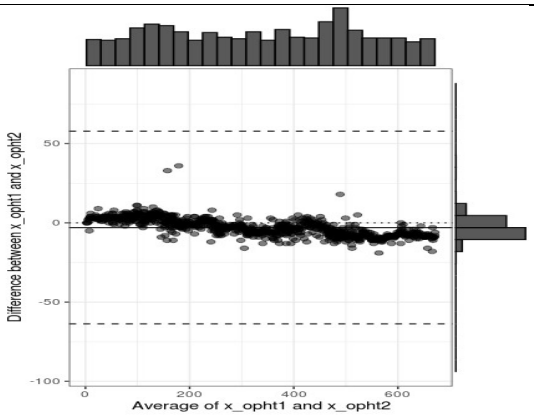

Figure 11. Correlation between the 1st and 2nd observation by the ophthalmologist coordinate Y in normal and altered funduscopies. R=0.96

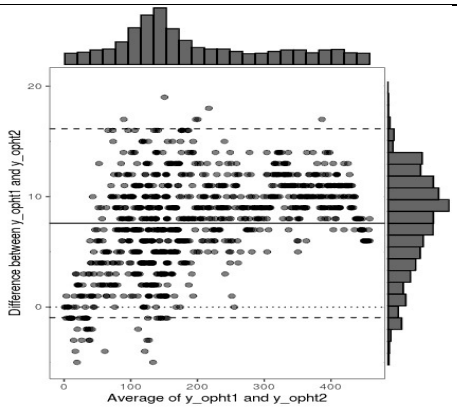

Figure 12. Degree of agreement between the 1st and 2nd observation by the ophthalmologist Y coordinate in normal and abnormal funduscopies

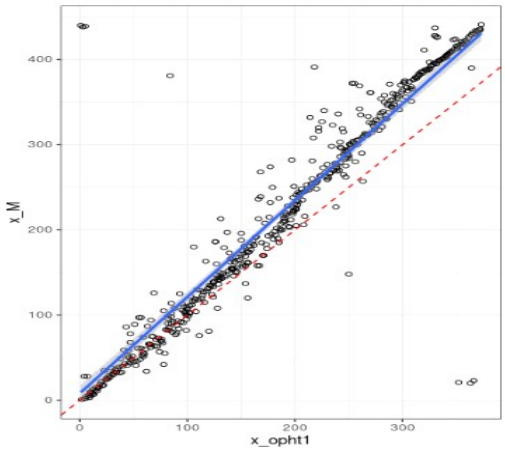

Figure 13. Correlation between the ophthalmologist's 1st observation versus 'X' coordinate machine in normal funduscopy. R=0.96

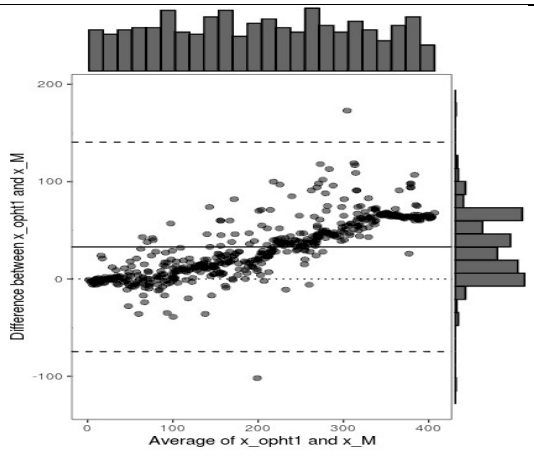

Figure 14. Degree of agreement between the ophthalmologist's 1st observation versus 'X' coordinate machine in normal funduscopies

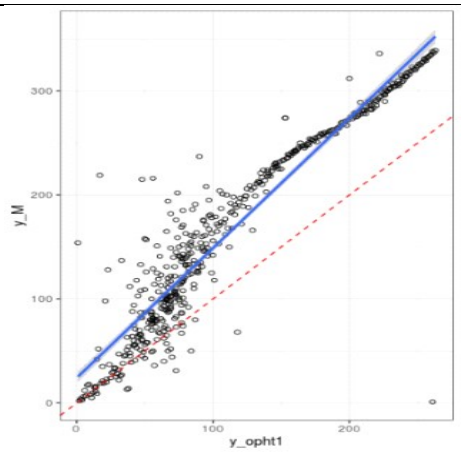

Figure 15. Correlation between the ophthalmologist's 1st observation versus 'Y' coordinate machine in normal funduscopies. R=0.96

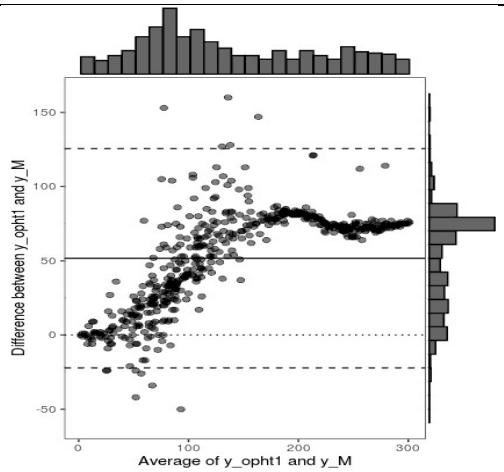

Figure 16. Degree of agreement between the ophthalmologist's 1st observation versus 'Y' coordinate machine in normal funduscopies

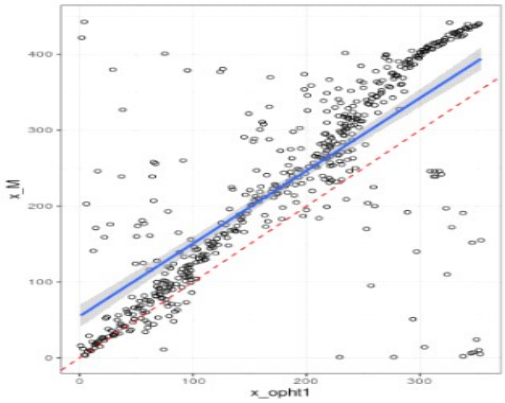

Figure 17. Correlation between the ophthalmologist's 1st observation versus 'X' coordinate machine in altered funduscopies. R=0.96

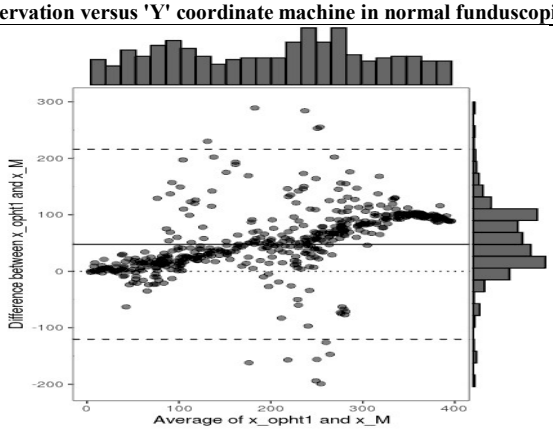

Figure 18. Degree of agreement between the ophthalmologist's 1st observation versus 'X' coordinate machine in altered funduscopies

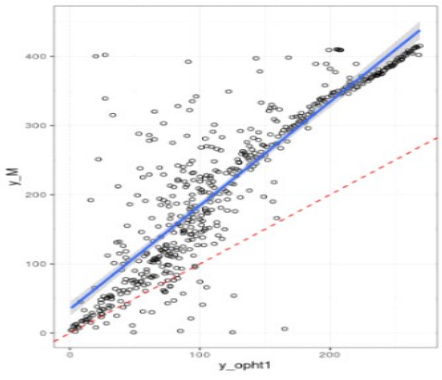

Figure 19. Correlation between the ophthalmologist's 1st observation versus 'Y' coordinate machine in altered funduscopies. R=0.96

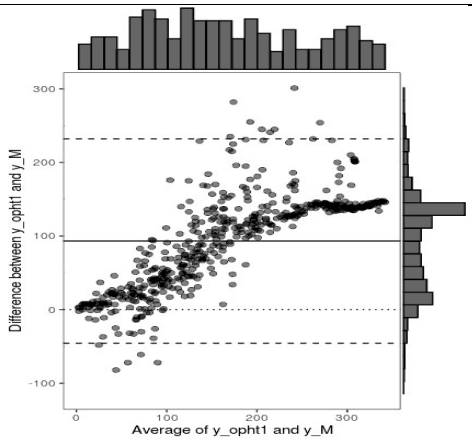

Figure 20. Degree of agreement between the ophthalmologist's 1st observation versus 'Y' coordinate machine in altered funduscopies

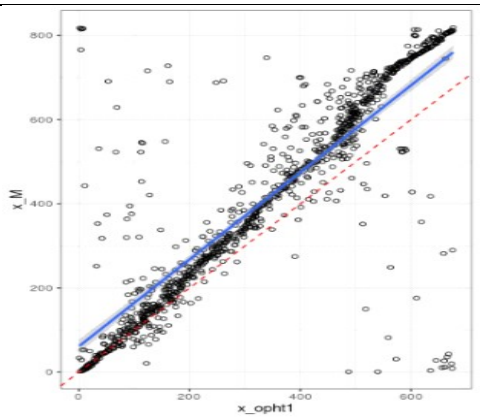

Figure 21. Correlation between the ophthalmologist's 1st observation versus 'X' coordinate machine in normal and altered funduscopy. R=0.96

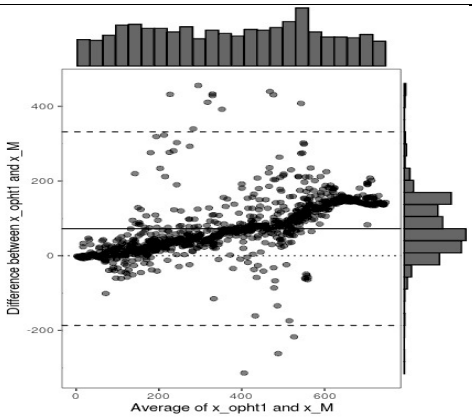

Figure 22. Degree of agreement between the ophthalmologist's 1st observation versus 'X' coordinate machine in normal and altered funduscopies. R=0.96

strong (Figure 19), the mean difference had a value of about 10 units above 0 (Figure 20). In the graphs of the 1st observation of the ophthalmologist versus the 'X' coordinate machine in normal and altered funduscopies, there was a strong correlation (Figure 21). The error size was approximately 75 units in the agreement analysis (Figure 22).

The graphs of the ophthalmologist's 2nd observation versus the 'X' coordinate machine in altered funduscopies had a strong correlation (Figure 29) and the mean difference was approximately 50 units above 0 (Figure 30). In the graphs of the 2nd observation of the ophthalmologist versus the 'Y' coordinate machine in altered funduscopies, the correlation was strong (Figure 31).

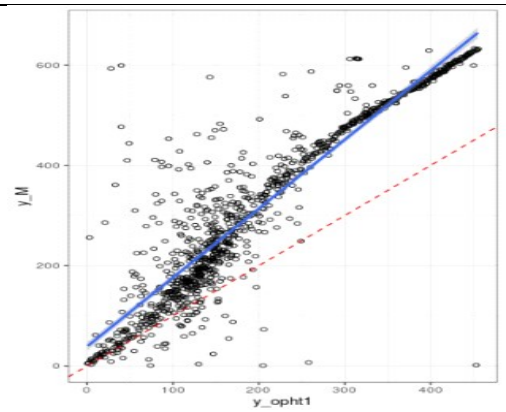

Figure 23. Correlation between the ophthalmologist's 1st observation versus 'Y' coordinate machine in normal and altered funduscopy. R=0.96.

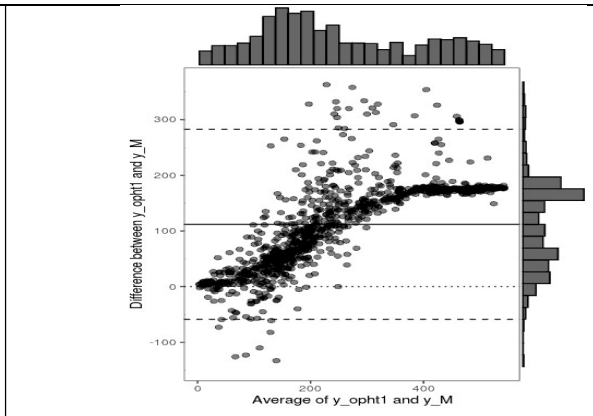

Figure 24. Degree of agreement between the 1st observation by the ophthalmologist versus the 'Y' coordinate machine in normal and altered funduscopies

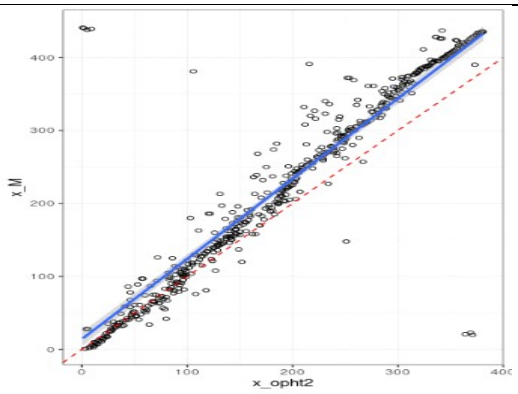

Figure 25. Correlation between ophthalmologist's 2nd observation versus 'X' coordinate machine in normal funduscopy. R=0.96

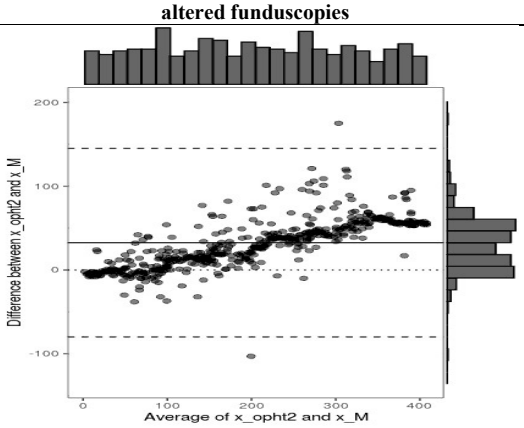

Figure 26. Degree of agreement between the ophthalmologist's 2nd observation versus 'X' coordinate machine in normal funduscopies

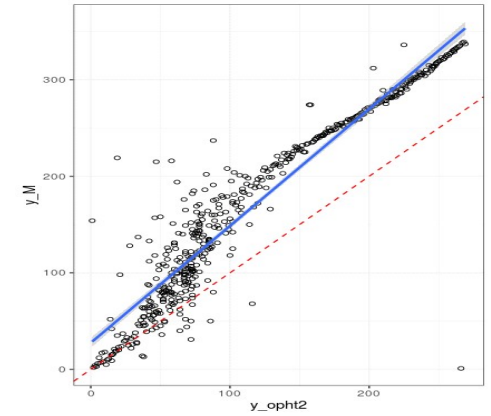

Figure 27. Correlation between the ophthalmologist's 2nd observation versus 'Y' coordinate machine in normal funduscopies. R=0.96

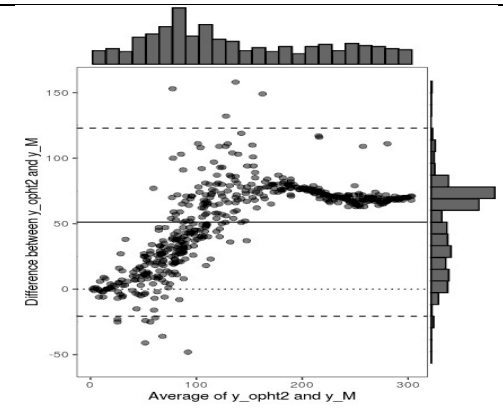

Figure 28. Degree of agreement between the ophthalmologist's 2nd observation versus 'Y' coordinate machine in normal funduscopies

In the graphs of the 1st observation of the ophthalmologist versus the 'Y' coordinate machine in normal and altered funduscopies, there was a strong correlation (Figure 23). The average difference exceeded 100 units far from 0 (Figure 24). The ophthalmologist's 2nd observation plots versus the 'X' coordinate machine on normal funduscopies had a strong correlation (Figure 25), and the error size was about 35 units above 0 (Figure 26). In the graphs of the ophthalmologist's 2nd observation versus the 'Y' coordinate machine in normal funduscopy the correlation graph was strong (Figure 27). The degree of agreement had an average difference of approximately 50 units (Figure 28).

The size of the difference between the observations was approximately 100 units (Figure 32). In the graphs of the 2nd ophthalmologist observation versus the 'X' coordinate machine in normal and altered funduscopies, the correlation was strong (Figure 33) and the mean difference of the observations was approximately 75 units above 0 (Figure 34). The graphs of the ophthalmologist's 2nd observation versus the 'Y' coordinate machine in normal together with altered funduscopies had a strong correlation (Figure 35), and the mean difference between the ophthalmologist's detection and the machine's detection was about 100 units above 0 (Figure 36). Figure 37 summarizes the discordance results according to fundoscopy group, coordinates and observers.

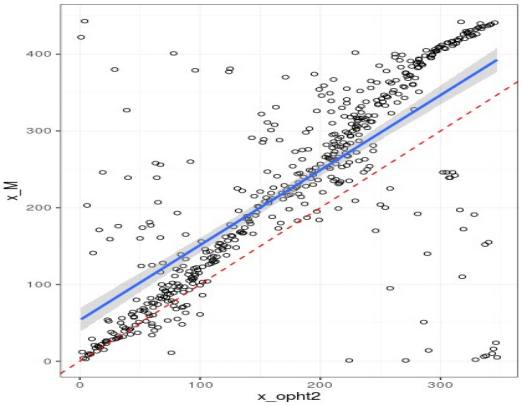

Figure 29. Correlation between the ophthalmologist's 2nd observation versus 'X' coordinate machine in altered funduscopies. R=0.96

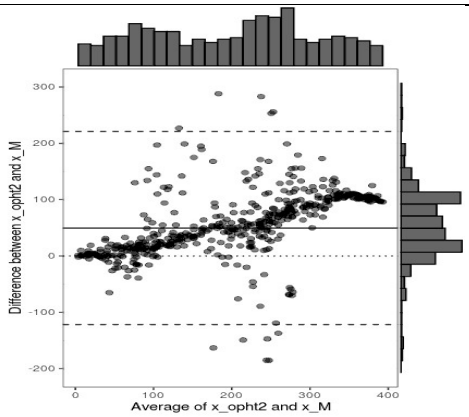

Figure 30. Degree of agreement between the ophthalmologist's 2nd observation versus 'X' coordinate machine in altered funduscopies

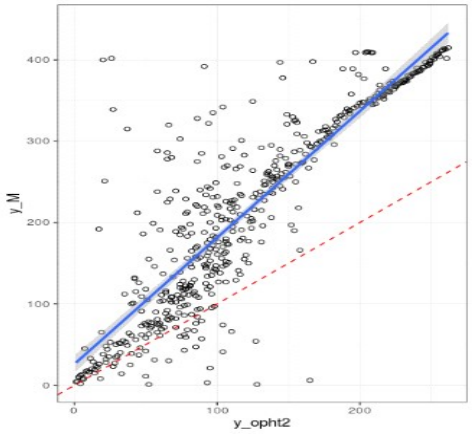

Figure 31. Correlation between the ophthalmologist's 2nd observation versus 'Y' coordinate machine in altered funduscopies. R=0.96

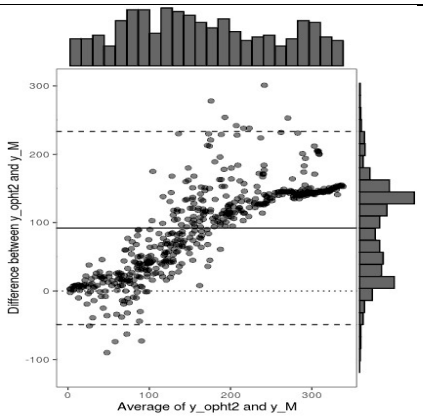

Figure 32- Degree of agreement between the ophthalmologist's 2nd observation versus 'Y' coordinate machine in altered funduscopies

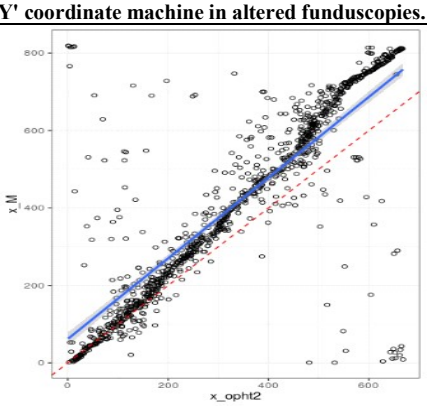

Figure 33. Correlation between the 2nd observation of the ophthalmologist versus 'X' coordinate machine in funduscopies together with altered ones. R=0.96.

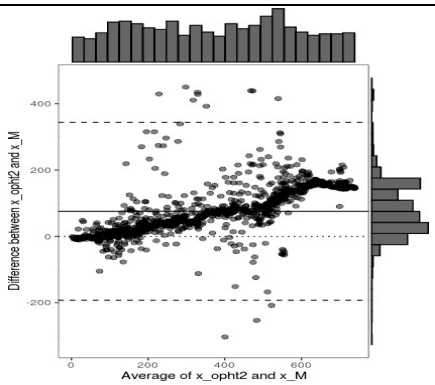

Figure 34. Degree of agreement between the ophthalmologist's 2nd observation versus 'X' coordinate machine in funduscopies together with altered ones

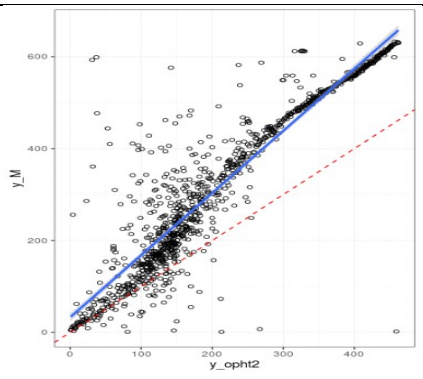

Figure 35. Correlation between the ophthalmologist's 2nd observation versus 'Y' coordinate machine in funduscopies together with altered ones. R=0.96

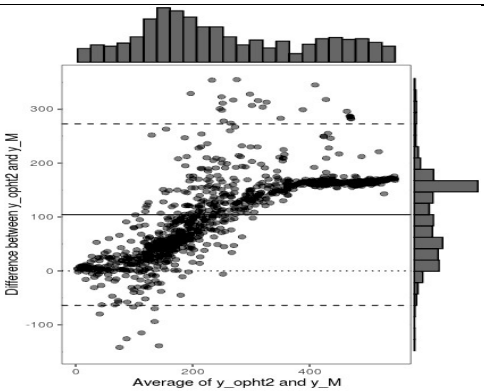

Figure 36. Degree of agreement between the ophthalmologist's 2nd observation versus 'Y' coordinate machine in funduscopies together with altered ones

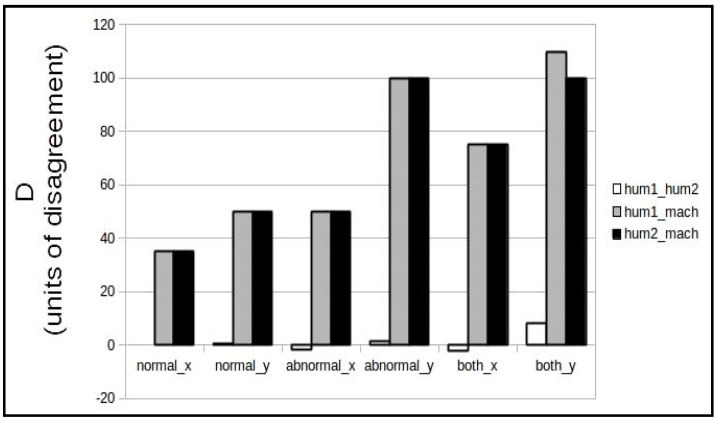

Figure 37. Mean difference units between coordinates, funduscopy groups and observers

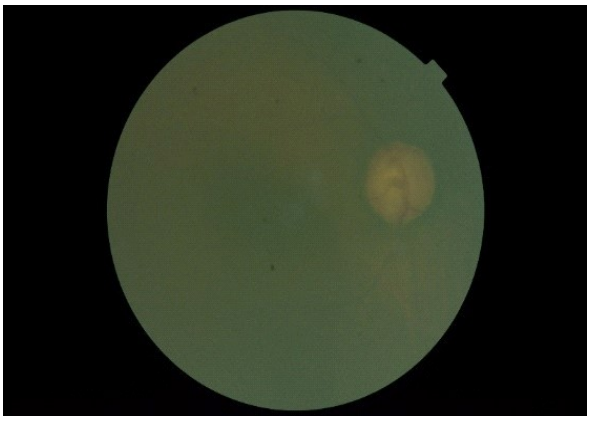

Figure 38. Retinography of the right eye that was not marked by the algorithm

Figure 39. Retinography of the right eye that was not marked by the algorithm

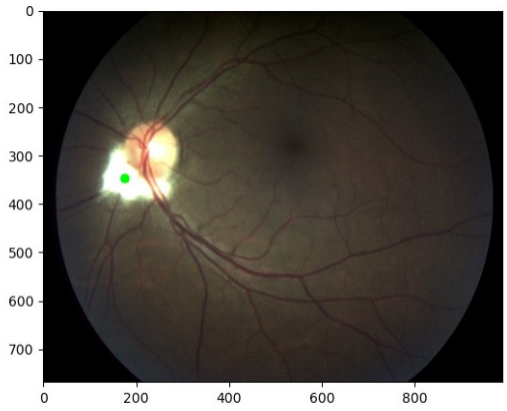

Figure 40. Retinography of the left eye in which the marking by the algorithm was outside the limits of the optic disc

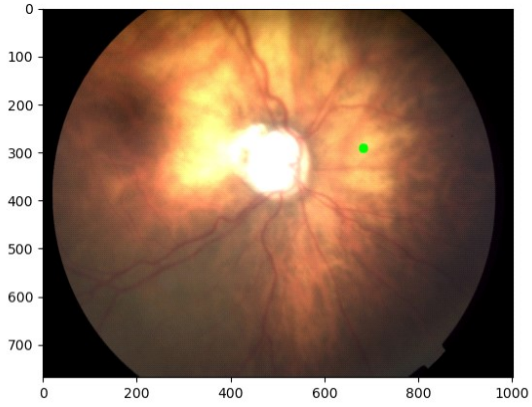

Figure 41. Retinography of the left eye in which the marking by the algorithm was outside the limits of the optic disc.

DISCUSSION

This study aimed to compare the performance of observations and markings of the optic disc center between an ophthalmologist and by computer vision through Bland-Altman analysis. Degrees of agreement were generated where it was possible to calculate the average difference in the size of the error between one observation and another. From this, it was seen that the 1st and 2nd observation of the same ophthalmologist had a strong degree of agreement in all coordinates, analyzing both normal, altered and normal funduscopy together with altered. The largest mean difference was about 8 units above 0, but all results are within the confidence interval. Similar to this, Fu et al.(24) proposed the segmentation of the optic disc and the excavation of the optic disc manually by 7 ophthalmologists in normal funduscopy and in funduscopies with glaucoma, and in optic disc segmentation there was little statistical difference (AUC between 0.89 and 0.85), while in the segmentation of the optic disc excavation there was a large statistical variation among ophthalmologists (AUC between 0.47 and 0.85). In the comparison of the two ophthalmologist's markings in relation to the machine's marking, it was seen that the average differences significantly increased all funduscopies groups both in the X coordinate and in the Y coordinate. mean differences reached 100 units above 0. It was noticed that the variation of what the machine detected as the center of the optic disc was greater when altered funduscopy and Y coordinate were involved, probably due to the difficulties of detection in images with low luminosity, blurring, low contrast and the pathologies themselves. Alshayeji et al.[25] in detecting the optic disc by the machine also found difficulties in some funduscopies and some

images were no longer marked, especially in funduscopies with poor optic disc contrast, with a lot of variation in backlighting, color similarity and contrast of the optic disc with the exudates of diabetic retinopathy. The location of the optic disc was also difficult in funduscopies with more pathologies. The identification and segmentation studies of structures are important, as they are the first step towards being able to use artificial intelligence in diseases that have specific biomarkers and lesions[26], as in the case of glaucoma. Automatic segmentation can also facilitate and optimize the conventional work of structural identification of the optic nerve[27], since manually it is very time-consuming[28]. For this reason, this work aims to analyze the performance of detecting the center of the optic disc by the machine, in order to arrive at the identification of glaucomatous optic nerves with this technology. Li et al.[29] studied the effectiveness of detecting optic disc neuropathy in glaucoma using normal and glaucoma funduscopy using deep learning technology with an n=48116, and showed a robust result, with AUC=0.986, sensitivity of 95, 6% and specificity of 92% in the detection of funduscopies referred to with glaucomatous optic disc neuropathy by the 21 specialists. During the choice of funduscopies, those with poor quality were excluded from the study.

The main reason for the appearance of false negatives (n=87) was the coexistence of other factors in the images, including pathological or high myopia. Likewise, Christopher et al.[30] had a high accuracy (AUC=0.91) in the identification of glaucomatous optic nerve (previously classified by a specialist., and even had a better performance in funduscopies with moderate to severe glaucoma (AUC=0.97) However, the inadequate quality of the retinography with blurring or low contrast can cause the model to generate errors and have low confidence results (AUC<0.5). In this study, only in 2 images the algorithm used could not identify and generate markings, which generated a good perspective for the model. The retinographies are represented in Figure 38 and Figure 39. In both images we can see the presence of blurring and a lower contrast, giving a homogeneous light intensity for the funduscopies. Although only 2 images were not identified by this model, some coordinates identified by the machine could not be inside the optic disc, as shown in Figure 40 that the optic disc is not represented as the brightest area of the image and in Figure 41 in that the marking of the coordinates was made at the second brightest point of the retinography. Liu et al.[31] also proposed the use of deep learning to identify glaucomatous optic nerves in different populations. The funduscopies used underwent quality control, which tried to reduce the images with significant artifacts, low resolution and inadequate lighting. In the local population (Chinese Glaucoma Study Alliance) the AUC reached 0.996, with a specificity of 97.7% and a sensitivity of 96.2%. In the other populations, there was an AUC greater than 0.964, specificity and sensitivity greater than 80.8% and 87.7%, respectively. When the model was used in different quality images obtained from the internet, the result was: AUC=0.823, Specificity of 70.4% and Sensitivity of 82.2%.

CONCLUSION

The study of the comparison of optic disc detection in funduscopies between a specialist and an AI algorithm allows us to conclude that the model used is promising. Some analyzes can be performed with the degrees of agreement generated by the Bland-Altman plots. When intra-specialist comparison was performed, the mean disagreement in all funduscopy and coordinate groups were similar and close to 0. Comparing the two observations of the ophthalmologist versus the machine, the disagreement between the two became evident as the mean differences increased. However, in some funduscopy groups, the detections of the optic disc center by the machine did not have unit discrepancies as strong as others. In funduscopies without pathologies, the detection of the machine tended to be closer to the markings made by the specialist in the two observations. The group of altered and normal funduscopies together with altered ones were where the disagreements were more accentuated. In addition, when the Y coordinate was involved, the discordances reached the highest unit values, reaching more than 100 units above 0. Therefore, there is a relationship regarding the coexistence of several factors present in the image, including pathological ones, in the performance of the model used. One of the factors that contributed to the increase in the mean difference was the luminosity of the retinographies, which is widely described in the literature. The algorithm used by the machine is also based on the illumination that the optic disc transmits, which can be confused with other light sources produced by certain pathological changes or impaired by inadequate image contrast.Despite a certain degree of disagreement between the specialist and the machine, the algorithm used in this study showed that it has great potential for detecting the center of the optic disc. The discussion around the various possibilities of investigation is necessary to increase the capacity of the model and make the difference between computer vision increasingly closer to an expert.

REFERENCES

Lopes A.A. Medicina Baseada em Evidências: a arte de aplicar o conhecimento científico na prática clínica. Rev. Assoc. Med. Bras. [Internet]. 2000 Sep [cited 2020 Mar 03] ; 46(3): 285-288. Available from: http://www.scielo.br/scielo.php?script=sci_arttext&pid=S0104-42302000000300015&lng=en. https://doi.org/10.1590/S0104-42302000000300015.

Ting, D.S.W., Peng, L., Varadarajan, A.V., Keane, P.A., Burlina, P., Chiang, M.F., Schmetterer, L., Pasquale, L.R., Bressler, N.M., Webster, D.R., Abramoff, M., Wong, T.Y., Deep learning in ophthalmology: The technical and clinical considerations, Progress in Retinal and Eye Research (2019), doi: https://doi.org/10.1016/j.preteyeres.2019.04.003.

Grewal, Parampal & Oloumi, Faraz & Rubin, Uriel & Tennant, Matthew. (2018). Deep learning in ophthalmology: a review. Canadian Journal of Ophthalmology. 53. 10.1016/j.jcjo.2018.04.019.

An Ophthalmologist's Guide to Deciphering Studies in Artificial Intelligence Ting, Daniel S.W.Lee, Aaron Y.Wong, Tien Y. et al. Ophthalmology, Volume 126, Issue 11, 1475 – 1479.

Rao, Chetan & Raman, Rajiv. (2019). Artificial intelligence applications for Ophthalmology: Current status. Nepalese Journal of Ophthalmology. 11. 1-4. 10.3126/ nepjoph.v11i1.25409.

De Fauw, J., Ledsam, J.R., Romera-Paredes, B. et al. Clinically applicable deep learning for diagnosis and referral in retinal disease. Nat Med 24, 1342–1350 (2018). https://doi.org/10.1038/s41591-018-0107-6

Siegfried K. Wagner, Dun Jack Fu, Livia Faes, Xiaoxuan Liu, Josef Huemer, Hagar Khalid, Daniel Ferraz, Edward Korot, Christopher Kelly, Konstantinos Balaskas, Alastair K. Denniston, Pearse A. Keane; Insights into Systemic Disease through Retinal Imaging-Based Oculomics. Trans. Vis. Sci. Tech. 2020;9(2):6. doi: https://doi.org/10.1167/tvst.9.2.6.

Edward Korot, Siegfried K. Wagner, Livia Faes, Xiaoxuan Liu, Josef Huemer, Daniel Ferraz, Pearse A. Keane, Konstantinos Balaskas; Will AI Replace Ophthalmologists?. Trans. Vis. Sci. Tech. 2020;9(2):2. doi: https://doi.org/10.1167/tvst.9.2.2.

Mohammadi, Mahdi & Al-Azab, Fadwa & Raahemi, Bijan & Richards, Gregory & Jaworska, Natalia & Smith, Dylan & de la Salle, Sara & Blier, Pierre & Knott, Verner. (2015). Data mining EEG signals in depression for their diagnostic value. BMC medical informatics and decision making. 15. 108. 10.1186/s12911-015-0227-6.

Kaushik S. (2019). Commentary: Linear discriminant score for differentiating early primary open angle glaucoma from suspects. Indian journal of ophthalmology, 67 (1), 81–82. https://doi.org/10.4103/ijo.IJO_1506_18

García-Gonzalo, Esperanza & Fernández-Muñiz, Zulima & Garcia Nieto, Paulino Jose & Sánchez, Antonio & Menéndez, Marta. (2016). Hard-Rock Stability Analysis for Span Design in Entry-Type Excavations with Learning Classifiers. Materials. 9. 531. 10.3390/ma9070531.

Tucker, Allan & Vinciotti, Veronica & Liu, Xiaohui & Garway-Heath, David. (2005). A spatio-temporal Bayesian network classifier for understanding visual field deterioration. Artificial

intelligence in medicine. 34. 163-77. 10.1016/j.artmed. 2004.07.004.

Jake VanderPlas. 2016. Python Data Science Handbook: Essential Tools for Working with Data (1st. ed.). O'Reilly Media, Inc.

Matthäus Pilch, Knut Stieger, Yaroslava Wenner, Markus N. Preising, Christoph Friedburg, Erdmuthe Meyer zu Bexten, Birgit Lorenz; Automated Segmentation of Pathological Cavities in Optical Coherence Tomography Scans. Invest. Ophthalmol. Vis. Sci. 2013;54(6):4385-4393. doi: https://doi.org/10.1167/ iovs.12-11396.

Scikit-learn: Machine Learning in Python, Pedregosa et al. , JMLR 12, pp. 2825-2830, 2011.

Smadja, David & Touboul, David & Cohen, Ayala & Doveh, Etti & Santhiago, Marcony & Mello, Glauco & Krueger, Ronald & Colin, Jesus. (2013). Detection of Subclinical Keratoconus Using an Automated Decision Tree Classification. American journal of ophthalmology. 156. 10.1016/j.ajo.2013.03.034.

Gulshan V, Peng L, Coram M, et al. Development and Validation of a Deep Learning Algorithm for Detection of Diabetic Retinopathy in Retinal Fundus Photographs. JAMA.2016;316(22):2402–2410. doi:10.1001/jama.2016.17216

Tabuchi, Hitoshi & Kamiura, Notake & Saitoh, Aumu & Isokawa, Teijiro & Matsui, Nobuyuki. (2014). Ophthalmological Examination Determination Using Data Classification Based on Support Vector Machines and Self-Organizing Maps. Journal of Japan Society for Fuzzy Theory and Intelligent Informatics. 26. 559-572. 10.3156/jsoft.26.559.

Tran, Bach & Ha, Giang & Vu, Giang & Vuong, Quan-Hoang & Ho, Tung & Vuong, Thu-Trang & La, Viet-Phuong & Ho, Toan & Nghiem, Kien-Cuong & Nguyen, Huong & Latkin, Carl & Tam, Wilson & Cheung, Ngai & Nguyen, Hong Kong & Ho, Cyrus & Ho, Roger. (2019). Global Evolution of Research in Artificial Intelligence in Health and Medicine: A Bibliometric Study. Journal of Clinical Medicine. 8. 10.3390/jcm8030360.

Livia Faes, Xiaoxuan Liu, Siegfried K. Wagner, Dun Jack Fu, Konstantinos Balaskas, Dawn A. Sim, Lucas M. Bachmann, Pearse A. Keane, Alastair K. Denniston; A Clinician's Guide to Artificial Intelligence: How to Critically Appraise Machine Learning Studies. Trans. Vis. Sci. Tech. 2020;9(2):7. doi: https://doi.org/10.1167/tvst.9.2.7.

Saito T, Rehmsmeier M (2015) The Precision-Recall Plot Is More Informative than the ROC Plot When Evaluating Binary Classifiers on Imbalanced Datasets. PLoS ONE 10(3): e0118432. https://doi.org/10.1371/journal.pone.0118432

Jun. (Mar, 3 2020). Deep Learning Algorithms https://medium.com/jun-devpblog/dl-1-learning-algorithms-and-basic-terms-of-dl-65d46ceb1b0[a]

Altman DG, Bland JM (1983). "Measurement in medicine: the analysis of method comparison studies". *The Statistician*. 32(3): 307–317.

FU, Huazhu et al. A retrospective comparison of deep learning to manual annotations for optic disc and optic cup segmentation in fundus photographs. Translational vision science & technology, v. 9, n. 2, p. 33-33, 2020.

Alshayeji, Mohammad et al. Optic disc detection in retinal fundus images using gravitational law-based edge detection. Medical & biological engineering & computing, v. 55, n. 6, p. 935-948, 2017.

Schmidt-Erfurth, Ursula et al. Artificial intelligence in retina. Progress in retinal and eye research, v. 67, p. 1-29, 2018.

Zheng, Yuanjie et al. Optic disc and cup segmentation from color fundus photograph using graph cut with priors. In: International Conference on Medical Image Computing and Computer-Assisted Intervention. Springer, Berlin, Heidelberg, 2013. p. 75-82.

Almazroa, Ahmed et al. Optic disc and optic cup segmentation methodologies for glaucoma image detection: a survey. Journal of ophthalmology, v. 2015, 2015.

Li, Zhixi et al. Efficacy of a deep learning system for detecting glaucomatous optic neuropathy based on color fundus photographs. Ophthalmology, v. 125, n. 8, p. 1199-1206, 2018.

Christopher, Mark et al. Performance of deep learning architectures and transfer learning for detecting glaucomatous optic neuropathy in fundus photographs. Scientific reports, v. 8, n. 1, p. 1-13, 2018.

Liu, Hanruo et al. Development and validation of a deep learning system to detect glaucomatous optic neuropathy using fundus photographs. JAMA ophthalmology, v. 137, n. 12, p. 1353-1360, 2019.

****